Published in final edited form as:
Science. 2019 November 08; 366(6466): 723–727. doi:10.1126/science.aax6832.

Direct observation of changing NO_x lifetime in North American cities

Joshua L. Laughner[1,*], **Ronald C. Cohen**[1,2,†]

[1]Department of Chemistry, University of California, Berkeley, Berkeley, CA 94720, USA.

[2]Department of Earth and Planetary Sciences, University of California, Berkeley, Berkeley, CA 94720, USA.

Abstract

NO_x lifetime relates nonlinearly to its own concentration; therefore, by observing how NO_x lifetime changes with changes in its concentration, inferences can be made about the dominant chemistry occurring in an urban plume. We used satellite observations of NO_2 from a new high-resolution product to show that NO_x lifetime in approximately 30 North American cities has changed between 2005 and 2014 in a manner consistent with our understanding of NO_x chemistry.

Nitrogen oxides (NO_x = NO + NO_2) play a critical role in air quality, affecting human and plant health both directly (1, 2) and indirectly through the formation of surface-level ozone (3) and particulate matter (4–6) as well as by influencing the radiative balance of the atmosphere (7). Combustion in vehicle engines or industrial processes is the main cause of anthropogenic NO_x emissions; consequently, most developed nations have taken steps to reduce anthropogenic emissions through new regulations and technology.

However, NO_x lifetime is nonlinearly dependent on NO_x concentration (8, 9); therefore, changes in atmospheric concentrations of NO_x because of emissions reductions will depend not only on the magnitude of the reduction but also on the chemical regime active within a given air mass. Theoretical calculations of NO_x lifetime versus concentration are shown for three different volatile organic compound reactivities (VOC_R) in Fig. 1. In the "NO_x-limited" regime (Fig. 1, region II), NO_x lifetime decreases with increasing concentration of NO_x, whereas in the "NO_x-suppressed" regime (Fig. 1, region III), the opposite relationship is observed.

Satellite observations of NO_2 have been used to directly infer a plume-average NO_x lifetime in urban and power plant plumes by calculating the e-folding distance for an NO_2 plume downwind of a source and converting this distance to a lifetime with the average plume wind speed (8,10,11). This approach has been used previously to show that the OH concentration

† Corresponding author. rccohen@berkeley.edu.
*Present address: Division of Geological and Planetary Sciences, California Institute of Technology, Pasadena, CA 91125, USA.
Author contributions: R.C.C. and J.L.L. jointly conceived the study, and J.L.L. executed it.

Competing interests: The authors declare no competing interests.

Data and materials availability: The BEHR product (13) is freely available. The code used in this work is available at (23), and intermediate data (line densities and fits) are available at (24).

in an urban plume varies with wind speed (8) and to examine spatial patterns in NO_X lifetime across the United States (11).

We used version 3.0B of the Berkeley High Resolution (BEHR) NO_2 product (12,13) to directly observe NO_X lifetime in ~30 North American cities. The BEHR product, with high-resolution daily NO_2 a priori profiles, was necessary to this study because previous work (14) has shown that daily, high-resolution profiles are necessary to simultaneously retrieve NO_2 vertical column densities (VCDs) and lifetimes to accuracies of 30% or better. We show that there are observable changes in North American urban NO_X lifetime and that these changes suggest a transition from the NO_X-suppressed to NO_X-limited regime. We examined the implications for ozone production and the relationship between trends in NO_X emissions and NO_2 VCDs.

To calculate the effective lifetime in each city's NO_X plume, we computed line densities along the downwind direction averaged over April through September in 3-year periods. Throughout this work, we refer to these periods by the middle year; for example, "2006" represents results from April to September in 2005,2006, and 2007. We focused on weekday (defined as Tuesday through Friday) lifetimes because the greater weekday NO_X emissions owing to heavy truck traffic (15, 16) mean weekday lifetime will have a greater effect on NO_X concentration and therefore air quality. Details of this method, including quality filtering, are provided in the supplementary materials (17). This method has been used successfully in numerous prior studies (8,10,11,18,19).

Of the 49 cities initially chosen, 12 had no valid fits during the study period. Three of the remaining 37 had no statistically significant change in NO_X weekday lifetime over the 2005–2014 time period studied (Houston, Texas; Salt Lake City, Utah; and Seattle, Washington). The remaining 34 cities were categorized by the shape of their lifetime trend over time: increasing, decreasing, concave up (CCU), or concave down (CCD). Of these 34, three cities (Chicago, Illinois; Detroit, Michigan; and Richmond, Virginia) had significant changes in lifetime but did not fit cleanly into these categories, and three were not included because they had only two good quality fits (Columbus, Ohio, increasing; Jacksonville, Florida, decreasing; and Tucson, Arizona, increasing).

Line densities and fits from specific 3-year periods that describe the shape of the trend are shown for one city from each group in Fig. 2. There are clear changes in the rate of decay of the line densities downwind of the city. The trends of all cities in these four groups are shown in Fig. 3. The lifetimes shown are normalized to each city's mean lifetime. In addition to the median normalized lifetime for each group (Fig. 3, black line), normalized lifetimes in key years for individual cities are shown in Fig. 3 as the diamonds. The individual years are such that each point for a given city is statistically different from the ones preceding and following it. Unnormalized lifetimes are presented in fig. S1.

Although the uncertainties of the absolute lifetimes are quite large (~30%), much of the error is likely correlated in between years (supplementary text), leading to smaller relative uncertainty in the trends. However, the fraction of the error that is correlated is not well characterized. To be conservative, we retained the absolute uncertainty when considering the

trends. The trends shown in Fig. 3 are statistically significant as determined with pairwise *t* tests, using the ~30% absolute error. Additionally, for approximately two-thirds of cities included, the difference in downwind decay was sufficiently large to identify visually in the line densities (figs. S7 to S11).

In theory, total NO_X lifetime is controlled by two processes: loss to nitric acid and loss to alkyl nitrates. These processes are in competition, with nitric acid dominating at high NO_X concentrations and alkyl nitrates dominating at lowNO_X concentrations. The exact crossover point depends on the VOC_R, HO_X production [$P(HO_X)$], and alkyl nitrate branching ratio (α).

A theoretical calculation of the dependence of NO_X lifetime on NO_X concentration and VOC_R for fixed $P(HO_X)$ and a is shown in Fig. 1. The theoretical behavior can be divided into three regions, identified in Fig. 1 by the background shading and Roman numerals. Region III, traditionally termed the "NO_X suppressed" or "VOC limited" regime, is characterized by decreasing NO_X lifetime with decreasing NO_X concentration. Loss of NO_X to nitric acid is the primary loss route in this regime. Region II, part of the "NO_X limited" regime, is characterized by increasing NO_X lifetime with decreasing NO_X concentration. Region I, also part of the NO_X limited regime at very low NO_X concentrations, once again has decreasing NO_X lifetime with decreasing NO_X concentration.

The turning points that define the regions occur because of shifts in the dominant chemical loss pathways. The minimum between regions II and III is the point at which the sum of losses to alkyl nitrates and nitric acid is at its maximum. Below this, loss to nitric acid slows. The maximum between regions I and II occurs because the model predicts an increase in RO_2 radicals below that NO_X concentration, causing the loss of NO_X to alkyl nitrates to accelerate.

If we assume that the changes in lifetime are driven entirely by changes in NO_X concentration, then it is straightforward to identify where on the lifetime curves in Fig. 1 each of the groups shown in Fig. 3 lie. Cities that exhibit a minimum or maximum in NO_X lifetime (Fig. 3, C and D, respectively) are straight-forward to locate on Fig. 1. The CCU shape of the lifetime trends for cities in Fig. 3C can be explained if these cities started in region III and crossed into region II after going through their minimum lifetime. Likewise, the CCD lifetime trends of cities in Fig. 3D can be explained if these cities began in region II and transitioned into region I. Cities with consistently increasing lifetimes (Fig. 3B) must lie entirely in region II because that is the only region with $\partial\tau/\partial[NO_X] < 0$. Cities with decreasing lifetime with time could fall in either region I or III; however, they must fall entirely in one region or another because they never show a significant positive slope of lifetime. The NO_2 columns for this group are consistently less than those of the CCU group (Fig. 4), suggesting that the decreasing lifetime group is further left in Fig. 1 than the CCU group. Because the CCU group has entered region II by ~2010, this suggests that the decreasing group must be in region I.

This simple interpretation, which assumes the dominant factor in changing lifetime is changing NO_X concentrations, is complicated by the fact that after 2010, there is no longer a

monotonic decrease in NO_2 columns (Fig. 4) (20). This suggests that either the changes in NO_x concentrations controlling lifetime are not represented in the average columns presented in Fig. 4 or that factors other than NO_x concentration control lifetime after 2010. As we will show, changing lifetime affects the proportionality between emissions and NO_2 columns; because the columns in Fig. 4 represent an average over circles with 50- to 100-km radii, an increase in the NO_x remaining downwind of the emission source owing to increasing lifetime could balance the decrease nearer the source, causing a net zero change in the average. If we consider other factors that might control lifetime, after 2010 when all cities are expected to be in regions I or II, our steady-state model predicts that a change of 1 to 2 s^{-1} in VOC_R would lead to a ~50% change in lifetime (fig. S6A).

Qualitatively, these trends in lifetime suggest that all North American cities have entered a NO_x-limited chemical regime by 2013 (Fig. 1, regions I and II). This is a plume-average chemical regime; there may be variations in the instantaneous chemical regime through-out the plume. Nevertheless, this has implications for future plans to control ozone production. The NO_x-limited regime is so named because NO_x is the limiting reagent in ozone production (21). Therefore, we predict that future controls on NO_x emissions, rather than VOC emissions, will be more effective in limiting plume-average ozone production for North American cities.

Our observations of changing NO_x lifetimes in North America also have implications for emissions constraints. One study (20) identified a discrepancy between the U.S. bottom-up NO_x emission inventory and trends in NO_2 VCDs over the United States. They found that after circa 2010, NO_2 VCDs stopped decreasing, whereas the bottom-up inventory shows a steady decrease in NO_x emissions. However, this assumes that the proportionality between emissions and NO_2 columns is fixed over the study period. Under steady-state conditions, the column density expected is related to the product of lifetime and emissions by

$$\begin{aligned} & E = k[\mathrm{NO}_x] \\ & \Rightarrow E = \frac{[\mathrm{NO}_x]}{\tau} \\ & \Rightarrow E \cdot \tau = [\mathrm{NO}_x] \end{aligned} \tag{1}$$

where E is the emissions, k is the loss rate constant, t is the lifetime, and $[NO_x]$ is the NO_x concentration. Above, we have shown that this is not true because variations in lifetime throughout the study period are of similar magnitude to that of the change in emissions being constrained (~30 to 50%). Crucially, we observed changes in lifetime after 2010, even though the precise cause of those changes is uncertain.

To demonstrate the effect of changing life-time, we used 12 cities that have at most one rejected weekday lifetime fit. This allowed us to have a nearly continuous record of their lifetime. We computed the mass of NO_x expected over each city as the product of the city's lifetime (Fig. 5B) and the NO_x emissions from the U.S. Environmental Protection Agency's Motor Vehicle Emission Simulator (MOVES) (Fig. 5A) for the county that contains the geographic center of the city. The result is shown in Fig. 5C. Nearly all of the top emitters show a flattening in predicted NO_x trends after 2010, with Chicago as the most notable exception.

In Fig. 5D, we compare the predicted columns from Fig. 5C with observed BEHR NO_2 columns. Accounting for the lifetime effect on the predicted columns better captures the rapid pre-2010 decrease in NO_2 columns seen by BEHR and improves, though does not fully capture, the immediate post-2010 flattening in the column trends. By 2012–2013, discrepancies between the observed and predicted columns become more substantial; this suggests that at this point, other factors—such as the increasing contribution of background NO_2 to urban plumes (fig. S3) (22)—play a dominant role in explaining the discrepancy between top-down and bottom-up emissions estimates. However, the better agreement between the predicted and observed column trends than the MOVES emissions and observed column trends demonstrates that changing NO_X lifetime cannot be ignored in top-down emissions estimates.

We saw significant changes in NO_X lifetime in North American cities that are of the same order as changes in NO_X emissions over the same time periods. The pattern of these changes suggests that NO_X-limited chemistry dominates North American urban plumes and also demonstrates that the change in NO_X lifetime must be accounted for when relating NO_X emissions and concentrations. Fully understanding the factors driving NO_X lifetime after 2010 will require new techniques. Given the importance of changing NO_X lifetime shown here, we hope that this work will spur other groups to pursue independent corroboration of these changes in lifetime through various methods, including high-resolution modeling efforts, meta-analyses of aircraft and ground-based data, and new, higher-resolution satellite products. The higher spatial resolution of TROPOMI (Tropospheric Monitoring Instrument) and upcoming geostationary satellites will provide more information on whether NO_X concentrations near sources are continuing to decrease and therefore driving NO_X lifetime changes, even though the average NO_2 columns are unchanging after 2010. High-resolution HCHO retrievals will improve our ability to track urban VOC chemistry from space and therefore infer changes in VOC_R relative to changes in NO_X.

This work also suggests that space-based observations of NO_X lifetime could provide valuable information about how the oxidative capacity of the atmosphere in North American cities changes over time. Previous work (8) used NO_X lifetime measured from space to infer plume-average OH concentrations; how-ever, that work focused on the megacity Riyadh, where loss of NO_X to nitric acid is the only meaningful loss pathway. By contrast, our work suggests that U.S. cities do have important alkyl nitrate chemistry. New methods will need to be developed to correctly account for the partitioning of loss NO_X between alkyl nitrates and nitric acid in order to take full advantage of this capability.

Supplementary Material

Refer to Web version on PubMed Central for supplementary material.

ACKNOWLEDGMENTS

The authors thank P. Romer for assistance with the steady-state model used to generate Fig. 1.

Funding: This work was supported by a NASA ESS Fellowship (NNX14AK89H), NASA grant NNX15AE37G, and the TEMPO project (SV3–83019). This work used the Cheyenne high-performance computing cluster (doi:10.5065/D6RX99HX) provided by NCAR's Computational and Information Systems Laboratory, sponsored

by the National Science Foundation. This research also used the Savio computational cluster resource provided by the Berkeley Research Computing program at the University of California, Berkeley (supported by the University of California, Berkeley, chancellor, vice chancellor for research, and chief information officer).

REFERENCES AND NOTES

1. Wegmann M et al., Exp. Toxicol. Pathol. 56, 341–350 (2005). [PubMed: 15945273]
2. Kampa M, Castanas E, Environ. Pollut. 151, 362–367 (2008). [PubMed: 17646040]
3. Haagen-Smit AJ et al., Plant Physiol. 27, 18–34 (1952). [PubMed: 16654433]
4. Pandis SN et al., Atmos. Environ. A 26, 2269–2282 (1992).
5. C. A. Pope 3rd et al., N. Engl. J. Med. 360, 376–386 (2009). [PubMed: 19164188]
6. Burnett R et al., Proc. Natl. Acad. Sci. U.S.A. 115, 9592–9597 (2018). [PubMed: 30181279]
7. Myhre G et al., Climate Change 2013: The Physical Science Basis. Contribution of Working Group I to the Fifth Assessment Report of the Intergovernmental Panel on Climate Change (Cambridge Univ. Press, 2013), pp. 659–740.
8. Valin LC et al., Geophys. Res. Lett. 40, 1856–1860 (2013).
9. Browne EC et al., Atmos. Chem. Phys. 14,1225–1238 (2014).
10. Beirle S et al., Science 333, 1737–1739 (2011). [PubMed: 21940891]
11. Liu F et al., Atmos. Chem. Phys. 16, 5283–5298 (2016).
12. Laughner JL et al., Earth Syst. Sci. Data 10, 2069–2095 (2018).
13. Laughner J, Zhu Q, Cohen R, Berkeley High Resolution (BEHR) OMI NO2-Native pixels, daily profiles, v5, UC Berkeley Dash, Dataset (2018); doi: 10.6078/D1WH41.
14. Laughner etal JL., Atmos. Chem. Phys. 16,15247–15264 (2016).
15. Murphy JG et al., Atmos. Chem. Phys. 7, 5327–5339 (2007).
16. Marr LC, Harley RA, Environ. Sci. Technol. 36, 4099–4106 (2002). [PubMed: 12380081]
17. Materials and methods are available as supplementary materials.
18. Lu Z et al., Atmos. Chem. Phys. 15, 10367–10383 (2015).
19. Liu F et al., Atmos. Chem. Phys. 17, 9261–9275 (2017). [PubMed: 29104586]
20. Jiang etal Z., Proc. Natl. Acad. Sci. U.S.A. 115, 5099–5104 (2018). [PubMed: 29712822]
21. Pusede SE et al., Chem. Rev. 115, 3898–3918 (2015). [PubMed: 25950502]
22. Silvern etal RF., Atmos. Chem. Phys. Discuss. 2019,1–26 (2019).
23. Laughner JL, behr-github/NAm-NOx-Lifetime: version 1.3 (2019); doi:10.5281/zenodo.3386680.
24. Laughner JL, Cohen RC, Supporting data for “Direct observation of changing NOx lifetime in North American cities”; doi:10.6078/D1RQ4V.

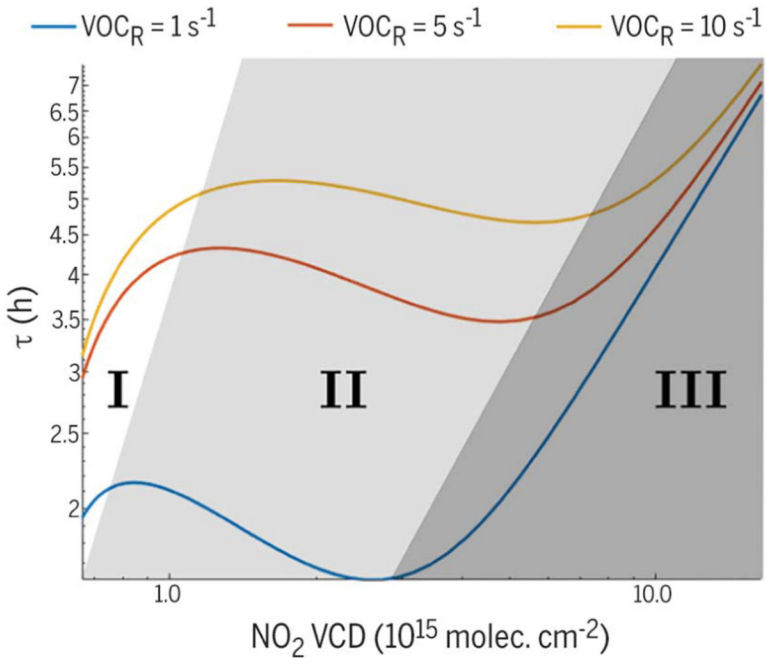

Fig. 1. Theoretical NO_x lifetime calculated assuming steady state for the HO_x family.

$P(HO_x)$ = 0.3 parts per trillion (ppt) s^{-1}, and the alkyl nitrate branching ratio α = 0.04. NO_2 VCDs were calculated from NO_x concentrations assuming a 1-km planetary boundary layer, a 4:1 NO_2:NO ratio, and a 5×10^{14} molecules cm^{-2} free tropospheric background NO_2 column. The Roman numerals and background shading identify regions used in the main text. VOC_R is volatile organic compound (VOC) reactivity, a measure of how quickly VOCs react with OH.

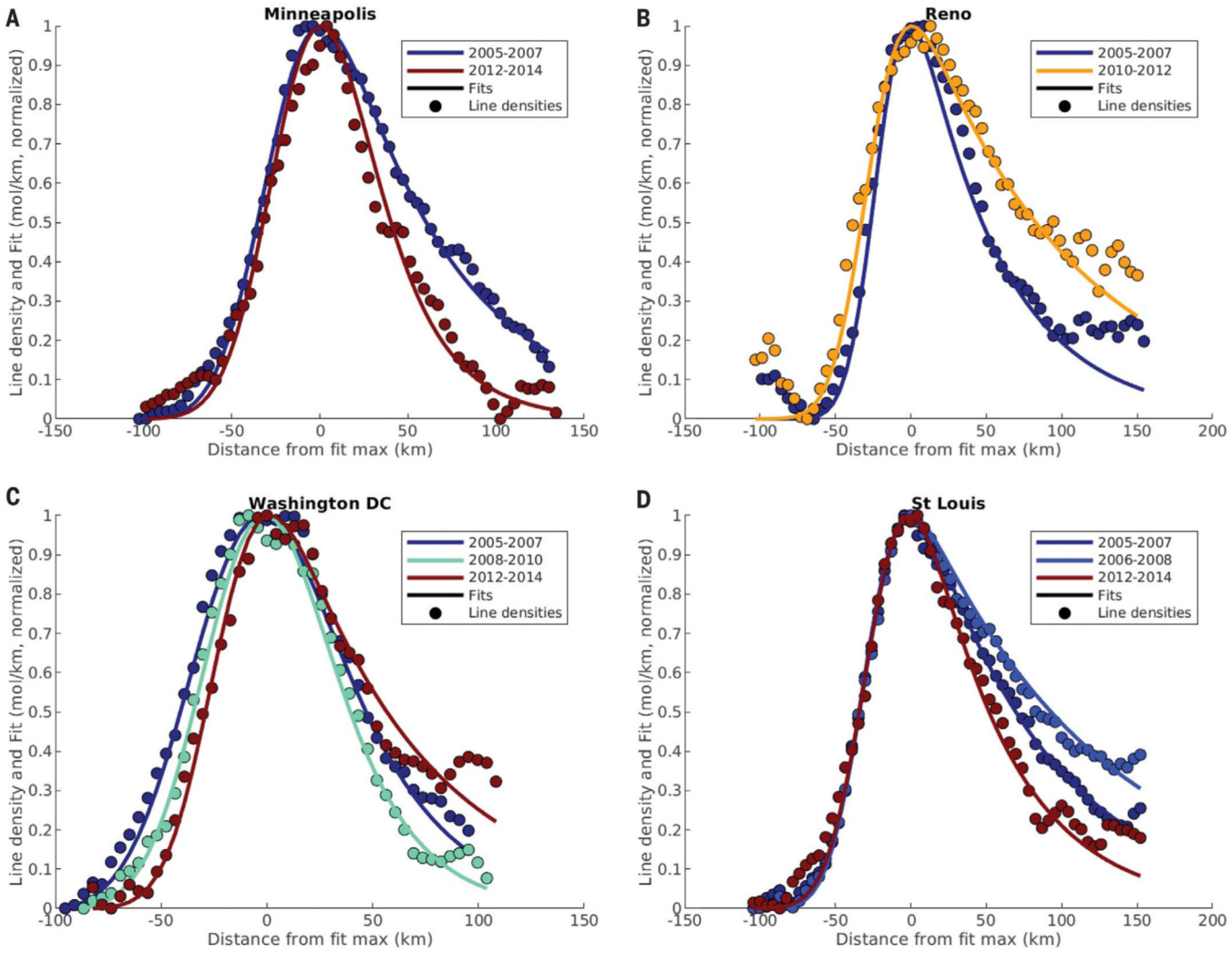

Fig. 2. Line densities and fits for four example cities, one from each group.

(**A**) Decreasing. (**B**) Increasing. (**C**) CCU. (**D**) CCD. Line densities are shown as circles, and fits are shown as solid lines. *y* axis values are normalized to a range of 0 to 1, and *x* axis values are positioned so that the maximum value of the fit occurs at 0.

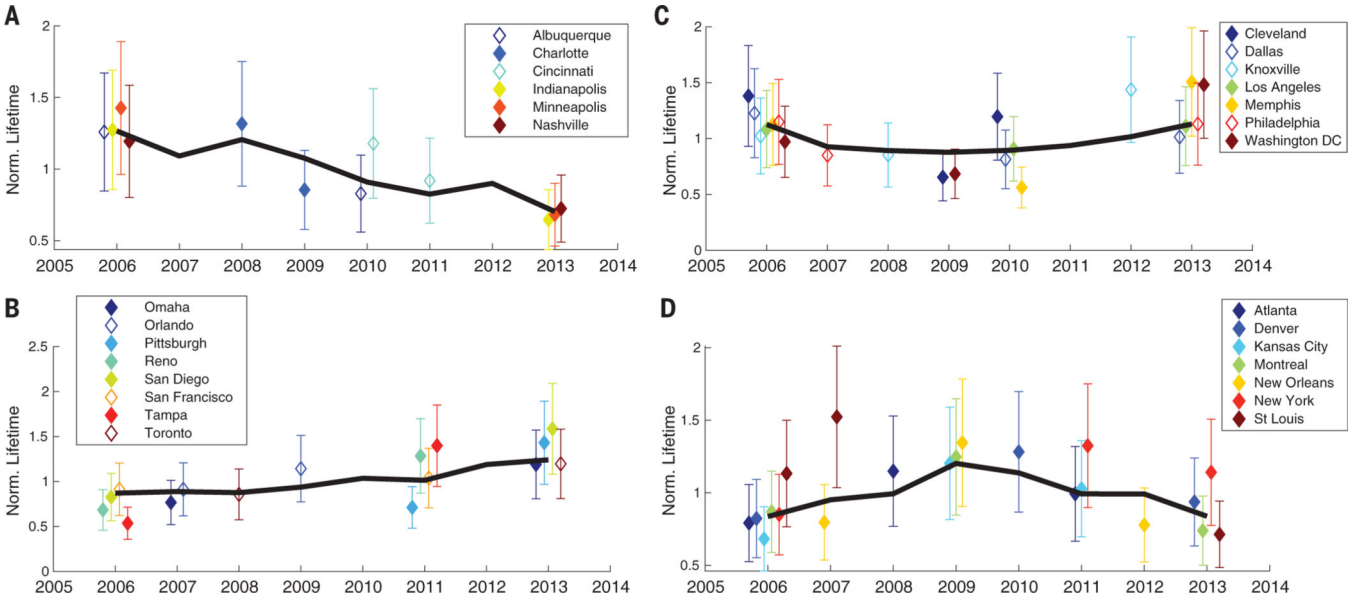

Fig. 3. Weekday (Tuesday through Friday) NO_X lifetime, normalized to each city's mean, for North American cities, divided into four groups based on the overall trend during the 2005–2014 time period.

(**A**) Decreasing. (**B**) Increasing. (**C**) CCU. (**D**) CCD. In (A) to (D), the black line indicates the median lifetime of the group, and the diamonds with error bars indicate individual lifetimes and their uncertainties for a city in a given 3-year period. Uncertainties are the absolute uncertainty in lifetimes. Open diamonds indicate cities that have statistically different fits, but the line densities have noticeable overlap between years.

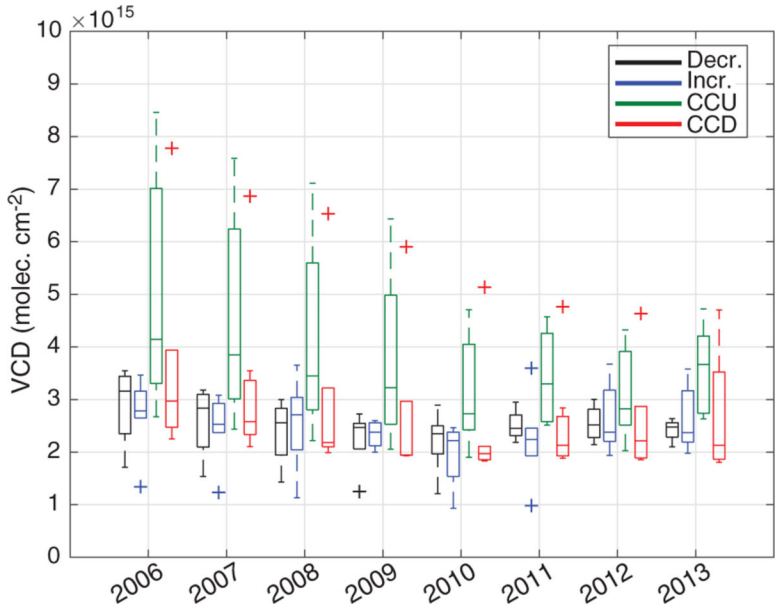

Fig. 4. Distributions of NO_2 columns for each of the four lifetime groups across the study time period.

For each box, the middle line indicates the median; the box top and bottom indicate the upper and lower quartiles, respectively; the whiskers indicate the farthest nonoutlier values; and plus (+) symbols indicate outliers.

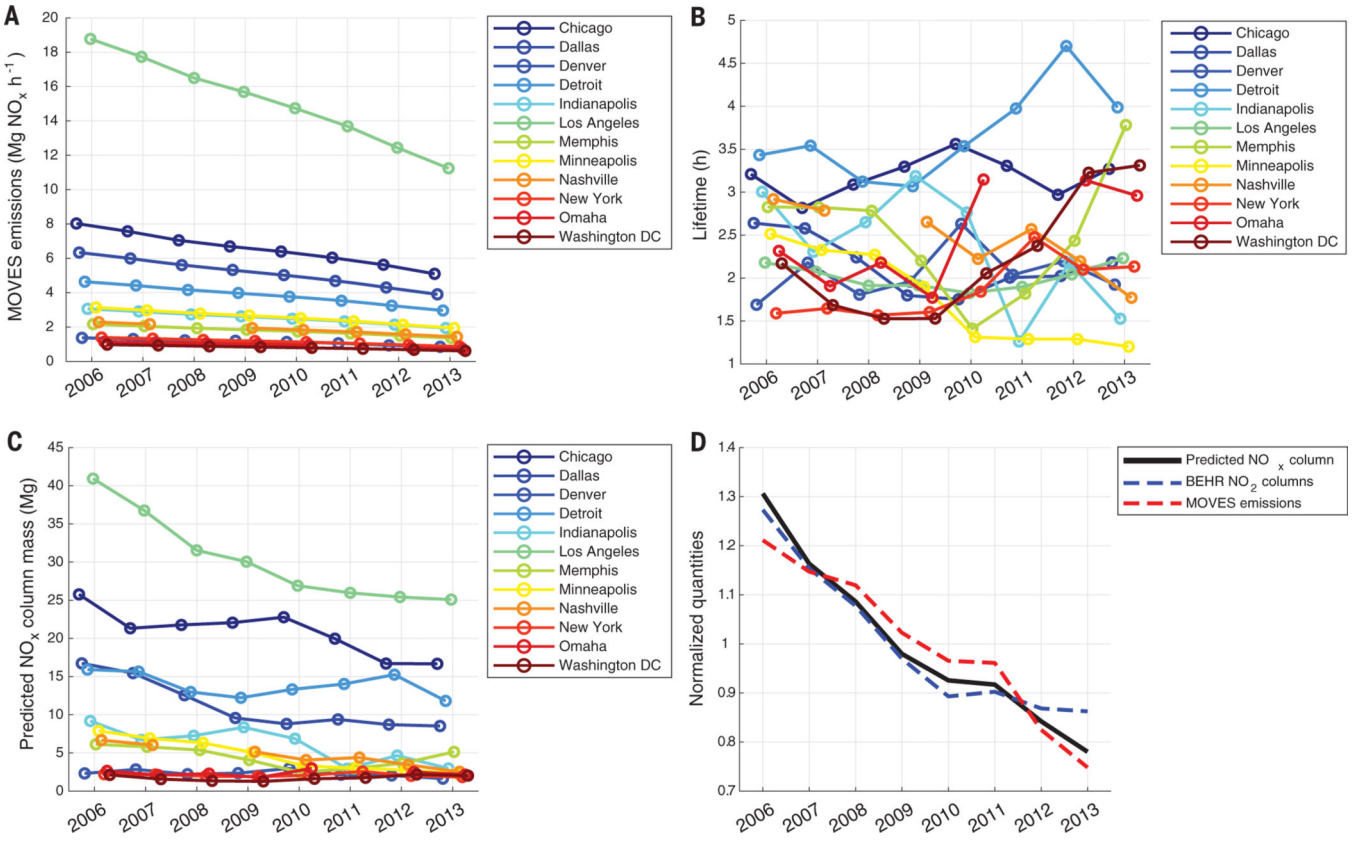

Fig. 5. NO_X emissions, lifetime, and predicted column mass for 12 United States cities.

(**A**) MOVES NO_X emissions for the core county of each of the 12 cities shown. (**B**) Lifetimes for the same 12 cities fit from BEHR line densities. (**C**) NO_X mass predicted for 12 cities as the product of their lifetime and MOVES NO_X emissions. (**D**) Trends in average NO_2 VCDs and MOVES NO_X emissions compared with the average predicted NO_X mass for the 12 cities in (C). Each series in (D) is normalized to its average.